Characterization of Water Vapor Plasma-Modified Polyimide

R. D. GOLDBLATT,[1,*] L. M. FERREIRO,[1] S. L. NUNES,[1] R. R. THOMAS,[1] N. J. CHOU,[1] L. P. BUCHWALTER,[1] J. E. HEIDENREICH,[1] and T. H. CHAO[2]

[1]IBM Research Division, T. J. Watson Research Center, Yorktown Heights, New York 10598
[2]State University of New York, Purchase, New York 10577

SYNOPSIS

To enhance polyimide-to-polyimide adhesion, we have investigated the effect of surface modification in water vapor plasma. The use of a water vapor plasma to treat a fully cured polyimide (PMDA–ODA) surface before subsequent layers of polyimide are applied results in dramatically enhanced interfacial adhesion. The polyimide-to-polyimide interfacial adhesion strength attained following water vapor plasma treatment exceeds the cohesive strength of the applied polyimide layer. The effect of surface modification in water vapor plasma on metal-to-polyimide adhesion has also been investigated. The use of a water vapor plasma to treat a fully cured polyimide (PMDA–ODA) surface prior to metallization results in increased metal-to-polymer interfacial adhesion. A study of both electroless and vacuum-deposited metal was conducted. The use of contact-angle measurements, peel tests, Fourier transform infrared spectroscopy, optical emission spectroscopy, nuclear forward scattering, and X-ray photoelectron spectroscopy has led us to a preliminary understanding of the resulting surface modification and the subsequent effect of adhesion promotion. © 1992 John Wiley & Sons, Inc.

INTRODUCTION

The use of polymers in the electronics industry has become pervasive. Many polymeric materials exhibit desirable bulk properties but have less than desirable surface characteristics. To tailor surface behavior to specific needs without altering bulk material properties, one may employ a variety of surface-modification techniques.

There are many ways in which polymer surfaces can be altered, but the techniques fall into two basic categories: physical and chemical modification. The use of physical modification (i.e., abrading, texturing, roughening, etc.) finds many applications as a means of adhesion enhancement in joining technologies, but for many polymer systems, the mechanical constraints of physical modification render its use inapplicable. Chemical modifications fall into

one of two categories: wet chemical and plasma surface modification.

Wet chemical modifications of polymer surfaces are employed to introduce new functional groups at the surface and in the near-surface region of the polymer. An example of this is the surface oxidation of polyethylene in chromic acid. The surface oxidation of low-density polyethylene has been analyzed by attenuated total reflectance-infrared spectroscopy[1] and X-ray photoelectron spectroscopy[2] and reveals the surface generation of carboxylic acids, ketones, and aldehydes. The chemical derivatization of these surfaces has been employed to create surface chemical species whose location and mobility may be studied using infrared spectroscopic reflectance techniques and electron spin resonance spectroscopy.[3]

In situations where one wishes to avoid wet chemical modifications or when it is desirable to confine a modification to the outermost hundreds of angstroms of a surface, plasma techniques may be employed. A great deal of research has been done

on the plasma modification of polymers and the subsequent surface analysis. The largest body of work deals with the plasma surface modification of polyethylene. Plasmas studied include argon and nitrogen plasmas[4-6] and air discharge,[7-12] which is also referred to as corona discharge. Included among the other systems studied are polypropylene and polystyrene surface modification in oxygen plasma,[13] poly(tetrafluoroethylene) treated in air discharge,[14] and poly(ethylene terephthalate) treated in air discharge.[15] To determine the resulting surface chemistry, X-ray photoelectron spectroscopy has been used immediately following plasma surface modification[7,8,11,13,14,16-19] as well as in conjunction with surface derivatization reactions following plasma treatment.[4-6,9,10,20] Clark and Harrison[21] even assembled a chart of core-level binding energies for common functionalities of interest in the study of polymers. The same as for a number of the studies on plasma surface modification, the aim of the work is to elucidate the effect of various plasma treatments on the adhesive properties of the polymer surface.[12,17,22-24]

The literature contains a number of works that have studied water vapor plasma.[25-31] Salvati et al.[32] proposed a mechanism that involves reactive decarboxylation/reduction followed by water chemisorption/functionalization for poly(methyl methacrylate) treated in a combination water vapor–argon plasma. After studying the plasma-modified surface with X-ray photoelectron spectroscopy, Fourier transform infrared spectroscopy, and low-energy ion-scattering spectroscopy, they concluded that the depth of modification was 50–100 Å and the primary resultant chemical species on the surface was —OH.

Ferreiro et al.[33] used a quadrupole mass spectrometer to sample the ions and neutrals from a radio-frequency-generated water vapor plasma. The major ions identified in a water vapor plasma are $H_2O^+\cdot$, H_3O^+, $O_2^+\cdot$, $H(H_2O)_2^+$, and $H(H_2O)_3^+$ at 43 milliTorr (mT) and 4 W. As the pressure is increased, the $O_2^+\cdot$ concentration increases due to collisionally induced decomposition of weakly bound clusters in the plasma sheath. This results in a higher concentration of atomic oxygen that makes a water plasma 40 times more efficient than an oxygen plasma for etching organic solids.

A number of different polymers have been subjected to water vapor plasma treatment and then studied. The effect of water vapor plasma on the adhesion of deposited cobalt on poly(ethylene terephthalate) has been examined.[34] The water vapor plasma treatment was shown to introduce hydroxyl

and carboxyl surface functionalities that resulted in improved wettability and increased adhesion. A study of the water vapor plasma treatment of polyethylene[35] using X-ray photoelectron spectroscopy shows the incorporation of hydroxyl moieties primarily as alcohols, with some hydroperoxides. X-ray photoelectron spectroscopy also determines the modification depth to be in the top tens of angstroms of the polymer surface.

Evans et al.[36] used angle-resolved electron spectroscopy for chemical analysis (ESCA, synonymously X-ray photoelectron spectroscopy) to study water vapor plasma modified polystyrene. Use of a reactor attached directly to an ESCA instrument allowed them to examine the plasma-treated surface without any contaminating exposure usually associated with transferring the sample from reactor to spectrometer. Surface oxidation products were identified as alcohols, ketones, ethers, peroxides, acids, esters, and carbonate functional groups. Variable angle ESCA estimated the thickness of the modified layer as 10–15 Å.

The goal of the current work is to use a water vapor plasma to create a polyimide surface that exhibits better adhesion to successive polyimide layers and to deposited metal. It will be shown that through the use of chemical derivatization following water vapor plasma treatment a variety of new surface chemistries may be created and explored.

EXPERIMENTAL

Instrumentation

The plasma system (shown in Fig. 1) consisted of a stainless-steel vacuum chamber with parallel plate electrodes. Prior to processing, the chamber was evacuated to a base pressure in the 10^{-7} Torr range using a 500 L/s turbomolecular pump. The plasma was generated between a grounded electrode (A) and an RF-powered electrode (B) attached to an 800 W, 13.56 MHz generator (F), through an automatic impedence matching network (E). The electrodes are 10 in. in diameter and separated by a 5 in. gap. During typical operation, 50 W of rf power was applied to the system. Samples were placed on the grounded electrode (A) and both electrodes had graphite cover plates. During processing, the system was pumped using a 30 cmh mechanical pump, and the pressure was monitored with a capacitance manometer (C). Water vapor was introduced into the chamber at point (D) using a heated liquid source (50–100°C) and a condensable vapor mass flow
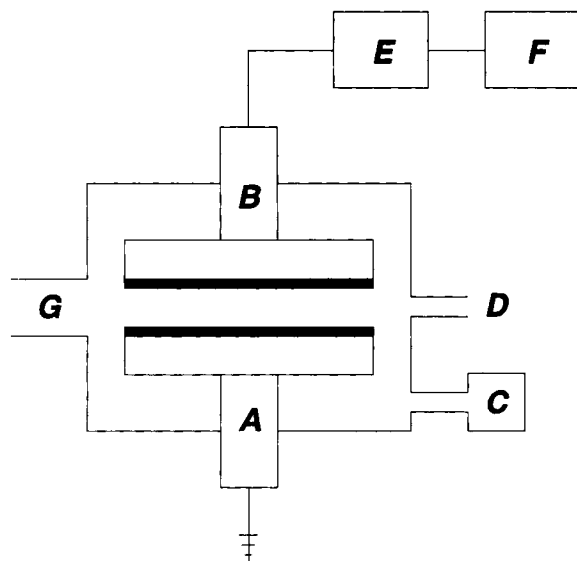
Figure 1 Plasma processing system: (A) grounded electrode; (B) rf-powered electrode; (C) capacitance manometer; (D) vapor inlet; (E) rf impedence matching network; (F) rf generator; (G) pumping port.

controller. All vapor transfer lines approaching the chamber were maintained at 100°C, and a refrigerated recirculator was used to maintain both electrodes at 25°C.

Metal vacuum deposition via electron-beam evaporation was done in a system specifically designed for that purpose. Evaporation rate was monitored with a quartz crystal and an Inficon Leybold-Heraeus (Syracuse, NY) crystal monitor. Metal sputter deposition was done using a Material Research Corp. (Orangeburg, NY) Model 903 planar magnetron metal deposition system.

Fourier transform infrared spectroscopy was performed on either an IBM IR-98 or an IBM IR-44 Fourier transform infrared spectrophotometer. Spectra were collected at 2 cm^{-1} resolution and were nominally an average of 500 scans.

Sample curing was done in one of the following: a Mellen (Penacock, NH) tube furnace with a flowing nitrogen environment or a Leybold Heraeus (Syracuse, NY) vacuum oven under a partial pressure of forming gas (200 mbar).

Temperature and humidity testing was carried out in an ESPEC (South Plainfeld, NJ) LH-112 humidity cabinet. A temperature of 85°C and a relative humidity of 81% were used as standard conditions.

Contact-angle measurements were made using the sessile drop measurement technique and a Rame-Hart (Mountain Lakes, NJ) NRL contact-angle goniometer Model 100 equipped with a tilting base, environmental chamber, and microsyringe attachment.

Film thicknesses were determined by ellipsometry with a Gaertner (Chicago, IL) variable-angle computer-controlled laser ellipsometer. For films thicker than 2 microns, a Sloan Technologies (Santa Barbara, CA) Dektak Model IIA surface profilometer was used.

Spin coating of sample films was done using a Headway Research (Garland, TX) Model AC201 photoresist spinner. Spin speed, spin time, and spin acceleration could all be controlled independently.

Peel testing utilizing a 90° peel angle was performed on one of the following: an MTS Systems Corp. (Guilford, CT) Model 812 Materials Testing System, an IMASS (Hingham, MA) Model SP-101B slip/peel tester, or a custom-built peel testing instrument.

X-ray photoelectron spectroscopy (XPS) experiments were carried out using a Surface Science Instrument small spot XPS tool, SSX-100-05, equipped with an AlKα X-ray source. Details of the analysis approach are given elsewhere.[37]

Atomic force microscopy (AFM) and nuclear forward scattering (NFS) experiments were performed at the IBM Thomas J. Watson Research Center using equipment specifically designed and built for that purpose. Details of both the AFM analysis[38] and the NFS technique[39] are given elsewhere.

Chemicals

Narrow dispersity polystyrene was purchased from Polymer Labs. Anhydrous sodium sulfate, HPLC-grade toluene, cupric sulfate, methyl isobutyl ketone, and sodium hydroxide were purchased from J. T. Baker Chemical Co. Formic acid, sodium salt (99+%), ethylenediaminetetraacetic acid (99.5%), HPLC-grade water, sodium potassium tartrate, malonyl dichloride (97%), chlorotrimethylsilane (98%), para-cyanobenzoyl chloride (98%), para-(trifluoromethyl)benzoyl chloride (97%), n,n-dimethyl benzylamine (99+%), nadic methyl anhydride (96%), and formaldehyde (37%) were purchased from Aldrich. Semiconductor-grade sulfuric acid and semiconductor-grade hydrochloric acid were purchased from Ashland Chemical Co. GAFAC surfactant was purchased from the GAF Corp. Plating additives HT1, HT2, and HT3 were purchased from Enthone (West Haven, CT). Polyimide (PI) films were prepared from DuPont Pyralin™ 2545 (an amic acid polymer prepared from 1,2,4,5-ben-

zenetetracarboxylic acid dianhydride (PMDA) and 4,4'-oxydianiline (ODA)).

The room temperature electroless copper bath was mixed as follows: 15.6 g $CuSO_4 \cdot 5H_2O$, 62.0 g NaK tartrate, 22.0 g NaOH, and two drops GAFAC, diluted to 1 L with DI water and activated with 7.5 mL/L of formaldehyde. The 72°C electroless copper bath was prepared as follows: 40 g ethylenediamine-tetraacetic acid, 20 g sodium sulfate, 20 g formic acid, 10 g $CuSO_4 \cdot 5H_2O$, and sodium salt, diluted to a volume of 1 L. The bath was activated with 2 mL/L formaldehyde prior to use.

The acid copper plating solution was prepared as follows: 270 g $CuSO_4 \cdot 5H_2O$, 351 mL H_2SO_4, 4.68 mL HCl, 15 mL HT1, 3 mL HT2, and 0.7 mL HT3 (Enthone Enplate™ Additives), diluted to 3 L with deionized water.

RESULTS AND DISCUSSION

Plasma Characteristics

The use of optical emission spectroscopy (OES) as a diagnostic technique for water vapor plasma processing was explored. Light collection was achieved with a fiber optical bundle. A grating monochromator and photomultiplier detector allowed collection of spectra from 280 to 850 nm. The use of a cutoff filter for wave lengths greater than 450 nm prevented second-order diffraction problems.

Water vapor plasmas were observed in the steady state at 10, 50, 100, and 200 W rf and at pressures of 100, 200, 350, and 500 mT. Integration of spectral intensities over the following regions were performed: OH band from 306.97 to 331.55 nm (this is the strongest set of bands), H atom line from 486.48 to 487.08 nm (the weaker of the two hydrogen lines that are consistently observed), CO bands from 513.45 to 520.95 nm (one of a set of three bands that are observed), H atom line from 656.70 to 657.30 nm (the strong hydrogen line), O atom line from 777.48 to 778.08 nm (the stronger of the two oxygen emission lines), and O atom line from 844.91 to 845.51 nm (the weaker oxygen line).

For all plasmas studied, the main emission features were the OH bands in the 306–331 nm range and the H atom lines at 486.1 and 656.3 nm. The integrated intensity of these emissions increased with increasing rf power at a given pressure, as did the low-intensity oxygen atom emission at 777.2 nm. CO emission was negligible except for runs performed in the extreme of highest power at lowest pressure. In the typical plasma operating regime, CO was not observed at a significant level.

From the emission studies of water vapor plasma, it is concluded that the main excited state species in the plasma are hydroxyl radicals and hydrogen atoms. A small amount of atomic oxygen is also observed. For the standard water vapor plasma operating parameters of 50 W rf at 185 mT, the excited state species present are hydroxyl radicals, hydrogen atoms, and a small amount of atomic oxygen. It is no surprise, then, that the major derivative observed following plasma modification is hydroxyl.

Surface Characterization

In initial attempts to elucidate the surface changes upon water vapor plasma treatment polystyrene was used as a model compound. Polystyrene ($\overline{MW}$ = 4,400,000; PDI = 1.06) was treated with water vapor plasma and examined. Typical plasma operating parameters were as follows: base pressure = 0.1–1 μT, electrode temperature = 25°C, vapor pressure = 100–300 mT, rf power = 50 W. Water contact-angle measurements using the sessile drop technique (0.05 mL advancing, 0.025 mL receding) revealed a significant change upon plasma treatment. The virgin polystyrene contact angles were measured to be 90 ± 2° advancing and 82 ± 2° receding. Water vapor plasma-treated polystyrene contact angles were measured to be 3 ± 2° advancing and less than 1° receding immediately following plasma treatment.

ATR–FTIR spectroscopic studies of polystyrene have been carried out. A sample of polystyrene film on a Ge ATR crystal was prepared by spin-coating a solution of narrow dispersity polystyrene (MW 8,000,000) in toluene, which was then baked at 90°C for 2 h. After being treated with water vapor plasma for 11 min, the sample gave an IR spectrum that has a new peak centered around 3665 cm^{-1} (Fig. 2).

Initial contact-angle experiments were repeated using PI. The water-contact angles, measured as described previously, for virgin 400°C cured PMDA–ODA were 65 ± 3° advancing and 45 ± 3° receding. Immediately following plasma treatment, these became 12 ± 2° advancing and 3 ± 2° receding.

FTIR spectroscopic studies of PI have been carried out on PI films spun and cured on germanium wafers or chromium-coated Si wafers, before and after water vapor plasma treatment, using both transmission and reflection–absorption FTIR spectroscopy. Following water vapor plasma treatment, a new feature in the IR spectrum is observed (Fig. 3) that has the same peak position and band contour as the OH peak observed previously in the IR spectrum of the water vapor plasma-treated polystyrene.
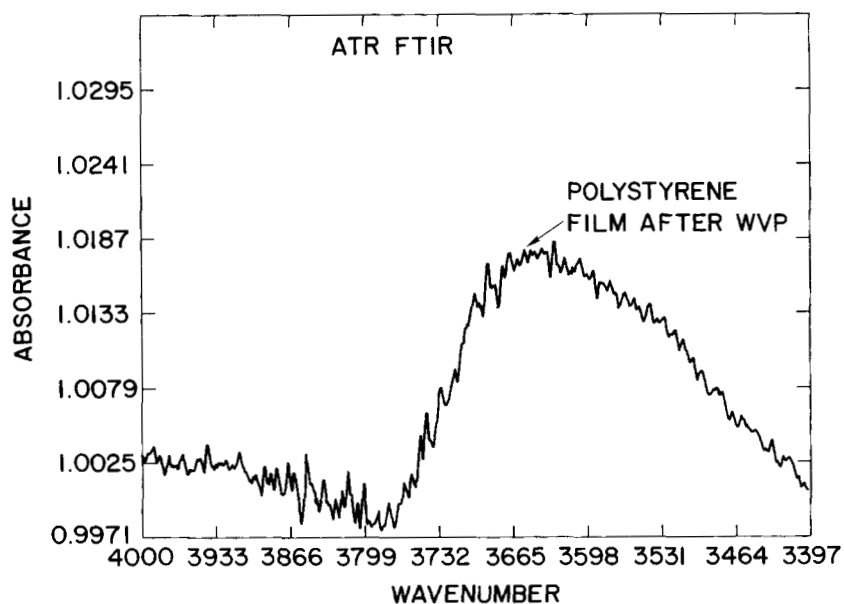
Figure 2   FTIR spectrum: plasma-treated polystyrene.

This experiment indicates that the plasma treatment on PI film generates a number of OH moieties on the film surface. Reproducible results have been obtained on PI films approximately 1000 Å thick treated with water plasma and etched to a final thickness of approximately 80 Å. A comparison of the IR reflectance spectra (Fig. 4) of a 900 Å unmodified film and a 70 Å modified film shows that the treatment resulted in a 30% decrease in the intensity of the 1740 cm^{-1} peak (C$=$O str.) normal-ized against the internal standard at 1503 cm^{-1} (1,4-phenyl ring str.) or 1244 cm^{-1} (C$-$O$-$C str.). This comparison, when made in the transmission mode, demonstrates no relative intensity decrease. It is further observed that the spectrum of a 1000 Å-thick film compared with that of an untreated 100 Å-thick film demonstrates no change or decrease in the ratios of the normalized intensities of the aforementioned peaks. If one considers that it is most likely near the substrate surface to have dipole moments of the
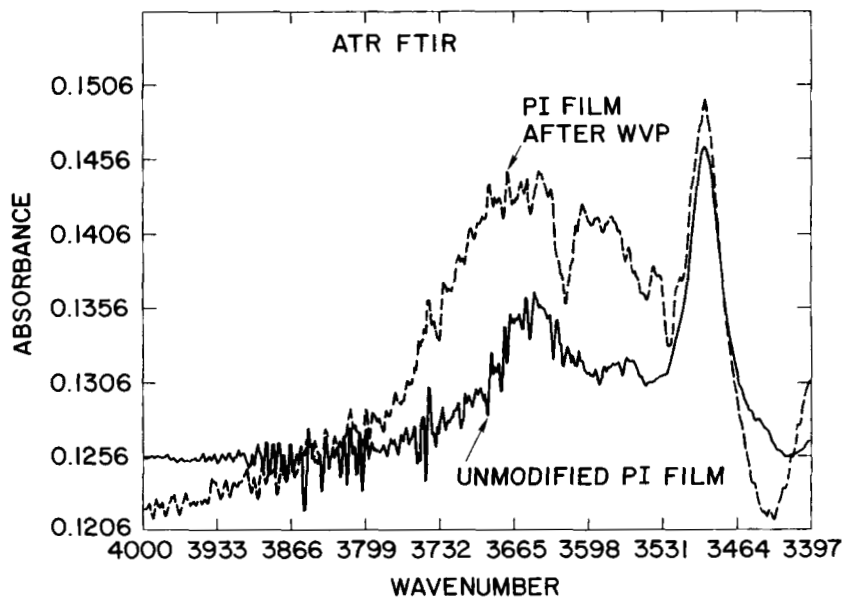

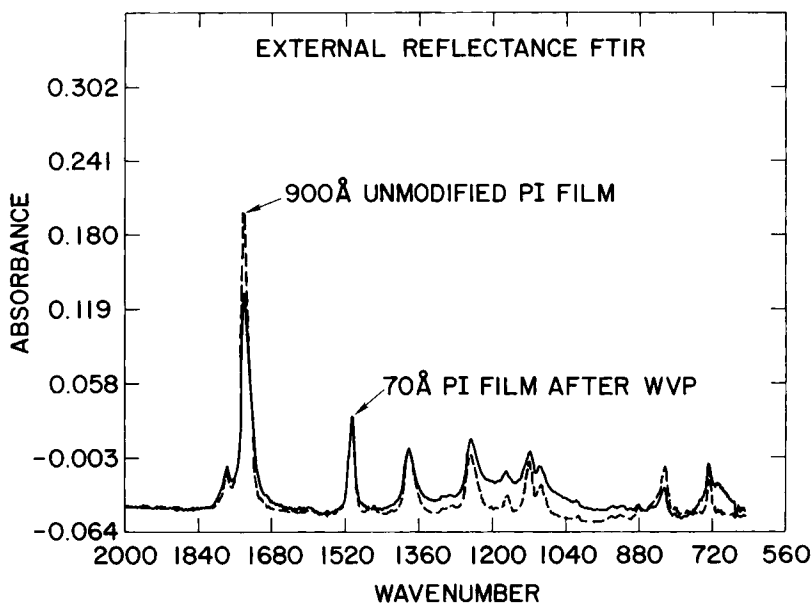**Figure 3**   FTIR spectrum: plasma-treated polyimide.

Figure 4   FTIR spectrum: plasma-treated polyimide.

C=O str. in plane for ordered regions of the PI, then if the water vapor plasma etch removes amorphous regions of the polymer at a greater rate rel-

ative to their ordered counterparts one would expect to see a relative decrease in the ratio of the normalized C=O str. intensity for the reflectance
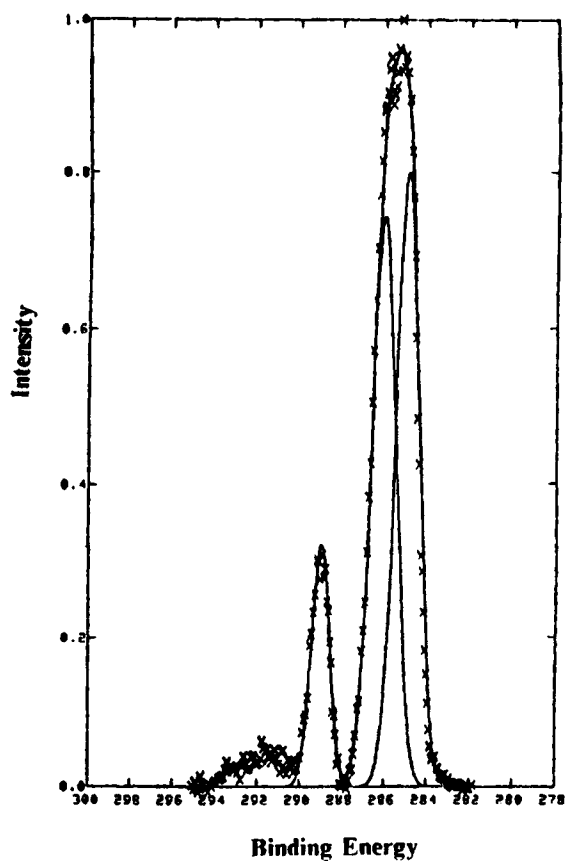

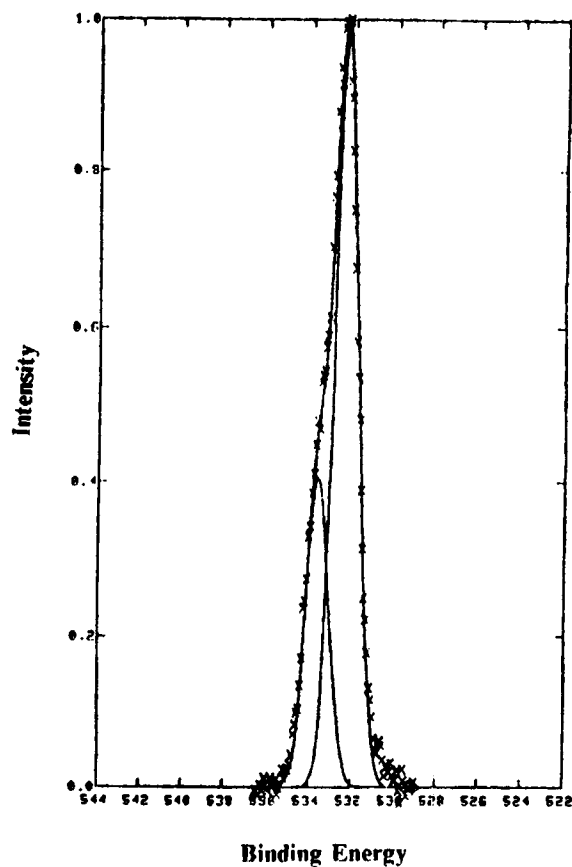**Figure 5**   XPS C 1s spectrum: PMDA–ODA control.

Figure 6   XPS O 1s spectrum: PMDA–ODA control.

FTIR compared to the transmission FTIR. This is precisely what was observed. This has led to the conclusion that the water vapor plasma treatment preferentially attacks the amorphous regions of the PI during the etch process.

To further elucidate the water vapor plasma-generated functionalities on PI films, a model compound, Parylene-N [(— CH_2 — C_6H_4 — CH_2 — $)_n$], was studied with FTIR. Oxygen-containing functional groups such as $C{=}O$, C — O — C, and C — O — H, if present after the plasma treatment, should be readily recognizable in the IR spectrum of Parylene-N. Samples of 1000 Å-thick films deposited on Cr-sputtered Si wafers were etched in the plasma to a final thickness of approximately 80 Å. External reflection–absorption IR spectra of the treated vs. untreated films showed that the treatment resulted in new carbonyl and hydroxyl groups as evidenced by the new peaks at 1743 (broad, $C{=}O$ str. vibration) and 1228 (broad, C — O str.) cm^{-1}.

The next analytical technique employed to characterize the water vapor plasma-treated PI surface was X-ray photoelectron spectroscopy (XPS). XPS results (Figs. 5–10) indicated a dramatic increase
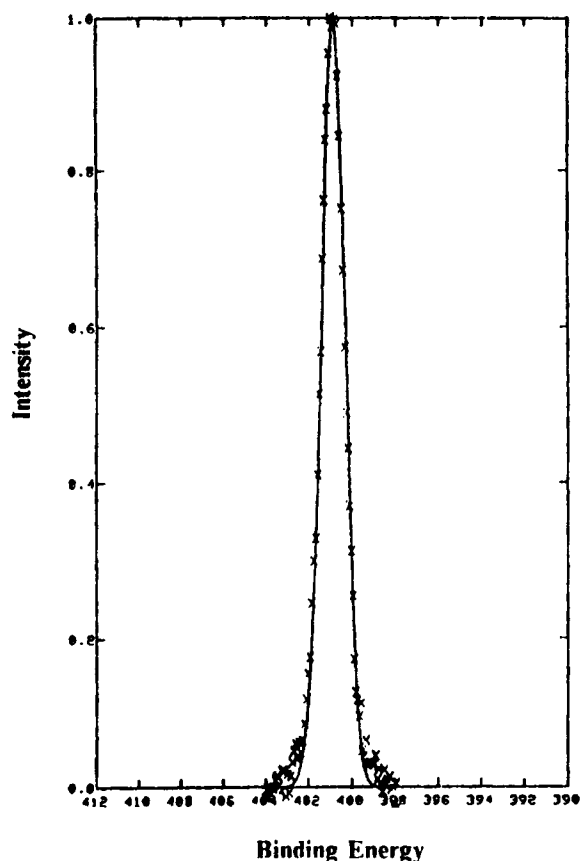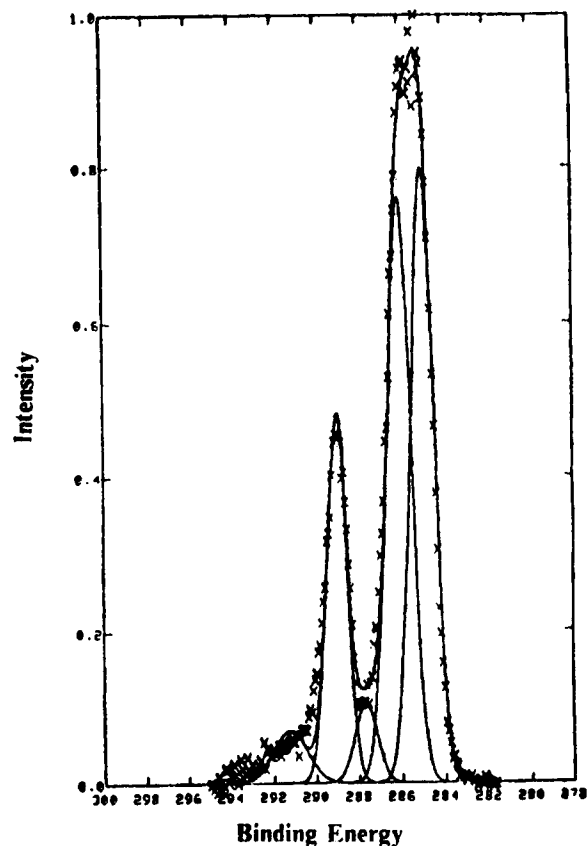

Figure 8 XPS C $1s$ spectrum: water vapor plasma-treated PMDA–ODA.

in the surface oxygen concentration following water vapor plasma treatment. An approximately 50% increase in oxygen concentration was observed. This oxygen was introduced primarily in the form of double-bonded and single-bonded species. The appearance of an acid/ester peak at 289.0 eV indicates either the occurrence of ring opening or the formation of additional carboxylic moieties during plasma treatment. Variable-angle XPS has led to the conclusion that the depth of modification is significantly less than 100 Å.

To further elucidate the characteristics of the modified surface, a nuclear forward scattering (NFS) study of water vapor plasma-treated PMDA–ODA polyimide was conducted. The NFS technique consists of bombarding the target specimen with a high-energy (2.3 MeV) $^4He^+$ beam at a glancing angle and measuring the energy spectra of the displaced hydrogen and deuterium atoms.[39,40] A mylar film is placed in the path to prevent $^4He^+$ from reaching the detector (mylar has a higher stopping power for helium than for hydrogen or deuterium). To minimize beam effects on the measured hydrogen or deuterium profiles, the NFS data from 10 separate 1
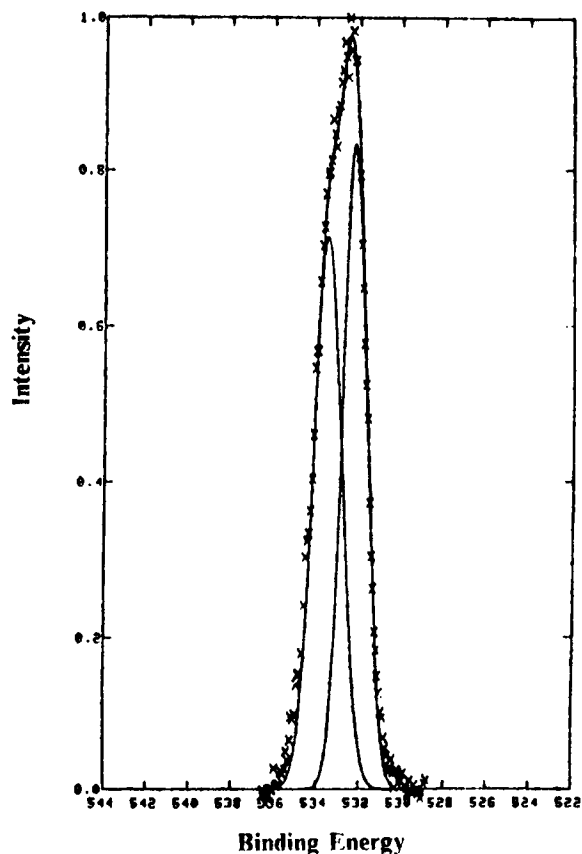

Figure 7 XPS N $1s$ spectrum: PMDA–ODA control.

Figure 9 XPS O 1s spectrum: water vapor plasma-treated PMDA–ODA.

X 1 mm spots on each specimen were summed to give a measured spectrum for that specimen. In anticipation of the possible hydrogen–deuterium exchange effect, all D_2O-treated samples were kept under D_2O ambient in the treatment chamber prior to their transfer for immediate scattering measurement.

From the NFS study of water plasma-modified PMDA–ODA PI surfaces, convincing evidence (seen as increased surface deuterium) was obtained that, under our processing conditions, the PI surfaces are deuteroxylated. The NFS data also indicated that after a long period of storage in a dry box the modified surfaces picked up a detectable amount of hydrogen, suggestive of a greater tendency for the treated surfaces to pick up ambient moisture than that for the fully cured films. Our results cannot rule out the possibility that a portion of detected hydrogen was from exchange of H_2O with any acidic deuteron present on the plasma-treated PI. The results of our study demonstrated that, when optimized, the NFS technique can provide important complementary information that will help resolve

the ambiguity in the results of other surface analytical techniques. In XPS studies of water plasma-modified PI surfaces, for example, increased oxygen coverage was observed, but the binding energy shift of O 1s and C 1s could be interpreted as the formation of either ketone or hydroxyl functionalities. The NFS technique helps resolve the ambiguity by monitoring the surface hydrogen concentration, which should increase with hydroxyl formation. As we found out in the course of our study, the technique has to be optimized with the use of deuterated specimens to appreciate the full advantage of the NFS technique.

To study the time-dependent behavior of the water vapor plasma-modified PI surface, sessile drop water contact-angle measurements were performed on a series of PMDA–ODA PI samples. The average observed contact angles for 400°C cured control samples are $67 \pm 3°$ advancing (Θ_{adv}) and $48 \pm 2°$ receding (Θ_{rec}). Immediately following water vapor plasma treatment, Θ_{adv} is $7 \pm 2°$ and Θ_{rec} is $3 \pm 2°$. When samples are allowed to stand in air for 1 week following water vapor plasma treatment, an increase
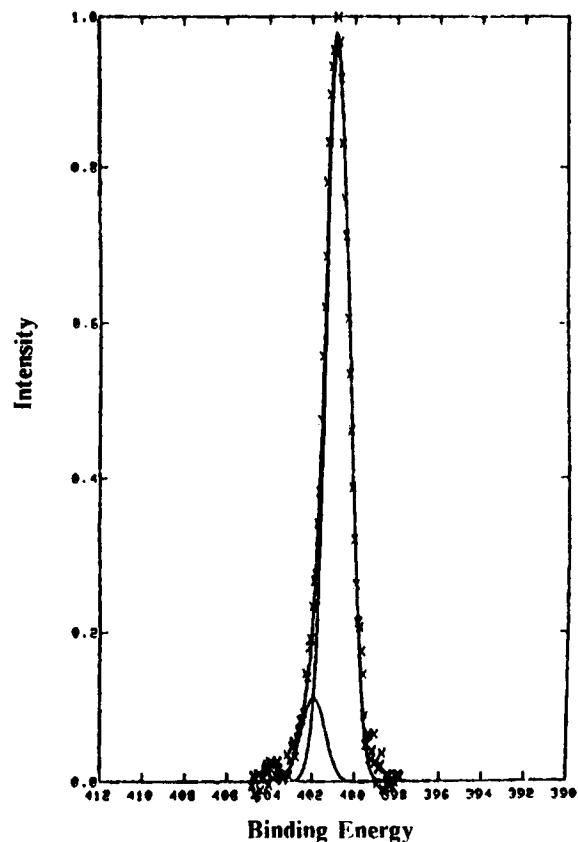

Figure 10 XPS N 1s spectrum: water vapor plasma-treated PMDA–ODA.

in Θ_{adv} and Θ_{rec} to $43 \pm 4°$ and $28 \pm 6°$, respectively, is observed. If samples are stored in vacuum following plasma treatment (without venting the chamber following treatment) or if samples are placed in water immediately, the contact angles are maintained at the low levels reported above. In all cases, the contact angles can be induced to change within the limits of the above values, depending upon the environment in which the surface is stored (Fig. 11). After repeated cycling between air and water conditions, the oscillations in the contact angles are damped, that is, some contact-angle hysteresis exists. Atomic force microscopy (AFM) measurements of the surface reveal an increase in surface topography (in the tens of angstroms range normal to the plane of the surface) following treatment in water vapor plasma (Fig. 12). After aging in air, this topography is observed to decrease and appears to be due to time-dependent surface reconstruction.

Based upon the above data, the following picture of the water vapor plasma-treated surface has emerged. During the plasma modification process, the PI surface experiences both chemical and physical changes. The observed plasma etch rate tells us that primary bonds in the polymer backbone are being broken. For the extreme case of etching, enough bonds are ruptured such that small backbone fragments are volatilized. During this process, it is reasonable to assume a steady-state surface configuration that makes the transition from the underlying unmodified PI to the outermost modified layers

that are the farthest along the progression toward removal. It is also logical to assume that during the etch process material is removed from the surface in a nonuniform fashion. Ordered regions will be removed more slowly than completely amorphous regions, and etching will occur the fastest along defect paths. This is in agreement with the AFM observed increase in topographical features following water vapor plasma treatment.

In consideration of the observed contact-angle hysteresis, the following is offered. During the plasma process, one effect of primary bond rupture is the generation of new chain ends. Chemical modification, i.e., hydroxylation of these free ends, results in an entirely new set of surface characteristics. The dramatic drop in contact angle following water vapor plasma treatment tells us that the excess surface free energy of the sample is increased upon treatment. It is then not surprising that in air the sample exhibits an increasing contact angle with time or, alternately, a decreasing excess surface free energy. The new surface created in the plasma contains "surface chains" that are not only more mobile than the bulk chains, but are also chemically different than their bulk counterparts. This is represented pictorially in Figure 13. The diffusion of these species back into the bulk serves to both minimize the excess surface free energy of the system, as well as to minimize the bulk free energy of the system as a result of the increased system entropy associated with surface desegregation. This may be reversed by
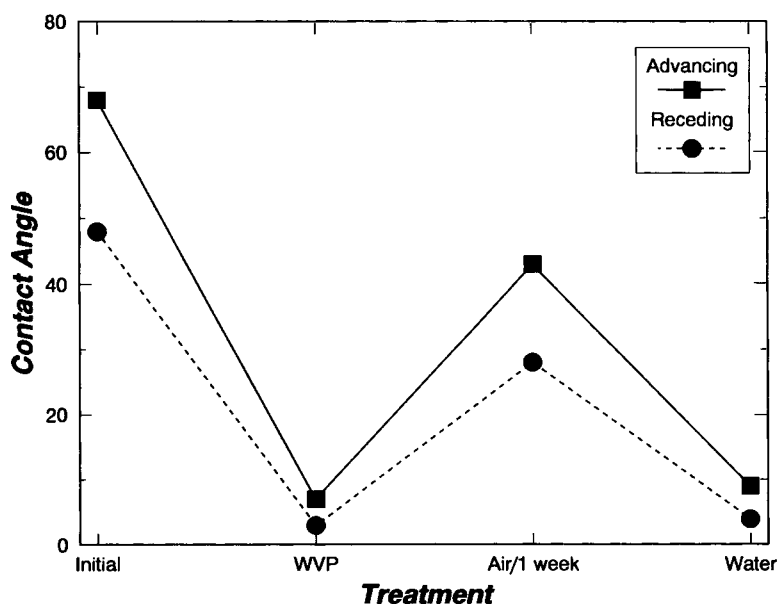

Figure 11 Time- and ambient-dependent contact-angle behavior of polyimide following water vapor plasma treatment.
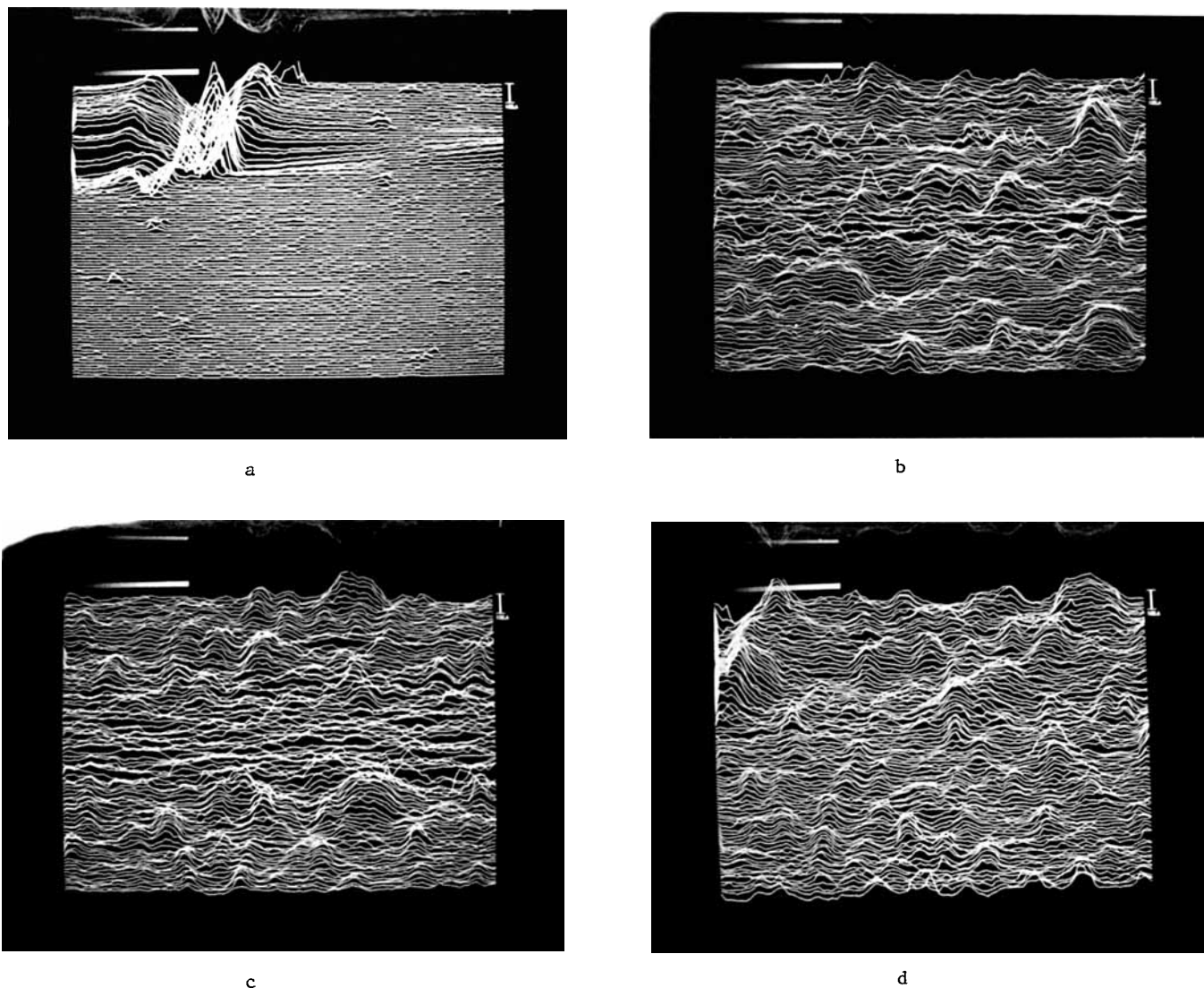
a

b

c

d

Figure 12   Atomic force micrograph: (a) control PI; (b–d) PI after water vapor plasma treatment.

submerging the sample in water, thereby causing the hydrophilic plasma-created species to migrate to the surface. The contact-angle hysteresis observed upon repeated cycling may be explained simply as increasing entanglement and therefore decreasing mobility of the "surface chains" as a result of their diffusion to and from the surface, induced by different external environments.

Similar variations in contact angle have been noted for homopolymers cast from different solvents and against different casting surfaces.[41,42] Additionally, the other effects of plasma-induced changes in the surface tension of PI should not be discounted. A change in surface tension or its measured variant, the contact angle, may be attributible to changes in

polymer molecular weight,[43-45] creation or exposition of chemically heterogeneous surfaces,[46] and/or surface roughening.[47] These factors and how they influence contact-angle studies on plasma-modified polymer surfaces are the subject of further investigation.

Polymer Self-Adhesion

Having gained this understanding of the effect of water vapor plasma, polymer–polymer adhesion testing was conducted. Test samples were prepared as follows: First, 500 Å Cr was e-beam evaporated onto Si wafers to provide an adhesive base. Wafers were then spin-coated with PMDA–ODA PI to a
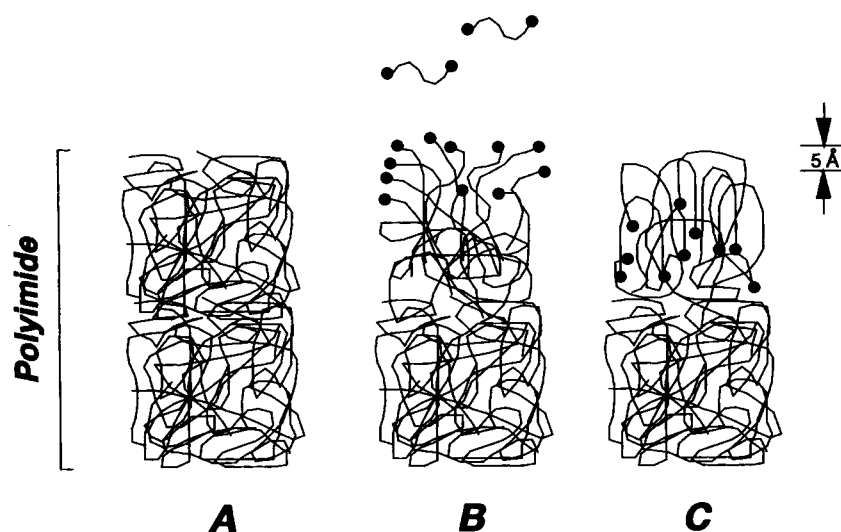
Figure 13 Polymer surface region: (a) control PI; (b) immediately following plasma treatment; (c) after elapsed time following plasma treatment.

post-400°C cure thickness of 5.5 ± 0.7 μm. An evaporation of 2.5 μm-thick copper on one edge of each wafer was then performed. This simplified the initiation of peel strips at the polymer–polymer interface later on. Samples were then separated into two sets: one control set and one set for water vapor plasma treatment. Following plasma treatment, both sample sets were spin-coated with PMDA–ODA PI, in multiple-coating steps, to a post 400°C cure thickness of 16.2 ± 2.1 μm. Five millimeter-wide peel test lines were initiated at the previously described copper release layer; 90° peel tests were performed using stroke-controlled peels at a rate of 4.55 mm/min. Peel test results for untreated PI control samples yielded a PI-to-PI peel strength of 5 ± 1 g/mm, whereas the water vapor plasma-treated samples yielded a PI-to-PI peel strength ≥ 90 ± 8 g/mm. This value actually represented the ultimate tensile strength of the peeling layer, which was exceeded prior to the observation of any interfacial adhesion failure.

To further define the useful range of applicability for water vapor plasma as a method of increasing PI–PI adhesion, an extended experimental matrix was run using the following experimental parameters: rf power: 50–200 W; run pressure: 50–300 mT; run duration: 5–35 min; elapsed time before post-plasma PI coating: 1–48 h. Peel testing at 90° revealed that for all plasma conditions employed the PI-to-PI interfacial adhesion strength exceeded the tensile strength of the 18 μm-thick PI layer. Numerically, this strength was greater than 125 ± 28 g/mm. After 1000 h of temperature and humidity

(T&H) testing (85°C/81% RH), this value dropped to 89.5 ± 11 g/mm, and the PI-to-PI interfacial adhesion strength remained greater than the tensile strength of the PI peeling layer.

Metal–Polymer Adhesion

For electronic applications, the ability to apply metal circuit patterns to a polymeric dielectric (specifically polyimide), and to do so in a manner that guarantees adequate adhesion, is essential. Further, in multilayer thin-film structures, the adhesion of metal conductors to polymer layers has to be durable enough to withstand all the processing required to build the layers. In addition, the metal/polymer interface has to be stable against thermal excursions that are needed to complete fabrication. Finally, since many of these structures are expected to function in nonhermetic environments, the adhesion has to be sustained through T&H cycles that simulate both the shipping and operating ambient exposures as well. Many simple schemes are available today to achieve acceptable metal/polymer adhesion at time zero. However, upon exposure to the thermal and T&H cycles described above, the interfacial adhesion tends to degrade noticeably. It is, therefore, very important to develop metallization procedures that yield strong and durable interfaces under these conditions.

As a measure of the relative magnitude of metal-to-polymer adhesion, 90° peel tests in which the metal is peeled of the polymer surface are performed. The results of our studies indicate that samples with

no water vapor plasma surface treatment had an evaporated Cr-to-fully cured PMDA–ODA PI adhesion of 2 g/mm, which is too low to be of any practical value. Water plasma-treated samples started with a peel strength of 50 ± 4 g/mm at time zero. After PI cure to 400°C, the adhesion values of treated samples were 52 ± 3 g/mm, in contrast to zero values in untreated samples. Peel strengths of treated samples were 44 ± 5 g/mm after exposure to 390°C. The adhesion was 48 ± 7 g/mm after five fast ramp thermal cycles to 350°C at 40°C/min.

On accelerated T&H testing for 675 h, after all the above temperature cycles, the average adhesion value for the water vapor plasma-treated samples was 30 ± 2 g/mm. After 1010 hours in the T&H chamber, these samples exhibited 24 ± 4 g/mm adhesion.

These results are superior to most data currently available for Cr/PI adhesion, which require the exposure of the polyimide to a high dose of inert gas ions (Ar, e.g., Ref. 48), particularly with regard to the durability of the adhesion. The proposed approach can be readily implemented in the currently used thin-film tooling. In fact, the use of a water plasma treatment is additionally attractive since such an exposure has been observed to promote PI/PI adhesion. Thus, such a treatment can be used to simultaneously accomplish metal/PI as well as PI/PI adhesion required in multilayer metal/polymer structures for microelectronic applications.

Electroless Copper

With the addition of oxygenated functional groups, especially those of the carboxylic acid type, the plasma-modified PI might be expected to behave as an ion-exchange resin.[49] Indeed, this has been observed experimentally. Water plasma-modified films have been shown to bind palladium ions (from an aqueous solution of the salt) in a process known as "seeding." This "seeded" surface could then be metallized in an elevated temperature electroless copper plating bath. A set of 400°C-cured PMDA–ODA PI samples was treated with a standard water vapor plasma. After seeding in aqueous palladium nitrate and electroless plating a strike layer, 15 μm-thick/2 mm-wide lines were electroplated in a standard acidic cupric sulfate bath. Ninety degree peel testing at a rate of 0.06 in./min revealed a Cu-to-PI peel strength of 47 ± 2 g/mm. This experiment was then repeated at a peel rate of 0.16 in./min, and 90° peel strengths were measured. For 25 μm final copper thickness, the resulting peel strength was 58 ± 8 g/mm.

Surface Functionalization

One way to overcome undesirable surface characteristics while preserving desirable bulk properties is to modify the surface, either chemically or physically, while leaving the bulk characteristics of the material intact. The continued investigation of the surface reactivity of water vapor plasma-treated PI has led to the execution of organic surface reactions that effectively tailor surface physical and chemical properties while maintaining desirable bulk characteristics.

The surface population of hydroxyl and carboxyl functionalities created on the polymer surface during water vapor plasma treatment have been targeted for grafting sites. The first reaction investigated utilized an acid chloride (malonyl dichloride) as the grafting reactant. Successful grafting was indicated by the observed change in sessile drop water-contact angle. Following water vapor plasma treatment, the water-contact angles were 19.5° ± 0.6° (advancing) and 3.5° ± 0.6° (receding). After allowing the malonyl dichloride to react with the surface, these angles were measured to be 62° ± 2° and 41° ± 2°, respectively.

To further demonstrate surface reactivity, the reagent chlorotrimethylsilane was used. The post-graft water-contact angles of 66° ± 4° (advancing) and 39° ± 3° (receding) indicate successful grafting. This was confirmed with XPS and the appearance, after grafting, of a silicon peak at 101.1 eV. Successful grafting, as determined by contact angle and XPS, has been achieved with the reagents *para*-cyanobenzoyl chloride and *para*-(trifluoromethyl)benzoyl chloride.

Perhaps the most interesting and useful surface graft examined was that of an epoxy resin with the reactive water vapor plasma-treated surface. For this purpose, a diglycidyl ether (DOW D.E.R. 667; bisphenol A-type resin; epoxide equivalent weight 1600–2000) was dissolved in methyl isobutyl ketone and allowed to react with the water vapor plasma-treated surface using *n,n*-dimethylbenzylamine as a catalyst. Successful grafting was observed by visual inspection and confirmed by both contact-angle measurements and by the observation of palladium "seeding" and copper plating using a conventional electroless copper plating bath. The ability of epoxy polymers to become activated toward electroless copper deposition is well documented.[50,51]

Utilizing the epoxy resin-grafted surface, we were able to further react the surface species by cross-linking with nadic methyl anhydride, again using *n,n*-dimethylbenzylamine as catalyst. This surface

could also be metallized with an electroless copper plating bath after palladium "seeding."

The ramifications of a PI with an epoxy surface are quite far reaching. The excellent bulk properties of PI coupled with the surface characteristics of an epoxy provide a technological advantage that would allow for the fabrication of a high-performance PI-based second-level package with a manufacturing scheme that could be implemented in a transparent fashion to any existing epoxy-based process scheme.

It is further anticipated that the diglycidyl ether graft can be used as an intermediate process, upon which subsequent grafting reactions may be executed. This allows us to create virtually any surface layer, with its associated characteristics, while leaving the bulk properties of the material upon which grafting has been accomplished intact.

CONCLUSIONS

Water vapor plasma surface modification of PMDA–ODA PI caused a significant increase in oxygen concentration as compared to the virgin surface. This added oxygen was primarily in the form of ketone, carboxylic acid, and hydroxyl groups. The effect of this surface modification on the strength of polymer–polymer adhesion was enormous. Polymer-to-polymer peel strengths measured following water vapor plasma consistently exceeded the tensile strength of the peeling layer before any interfacial failure was observed. Additionally, these polymer-to-polymer interfaces remained stable after more than 1000 hours of temperature and humidity ($85°C/81\%$ RH) testing.

The effect of water vapor plasma on metal-to-polymer interfacial adhesion and adhesion durability was dramatic. The metal-to-polymer interfaces continued to exhibit enhanced adhesion durability under conditions of accelerated temperature and humidity testing.

Data obtained from the OES work establish the presence of hydroxy radicals in the water vapor plasma. Upon consideration of the enhanced surface oxidation observed via XPS coupled with the NFS result of increased surface protonation/deuteration, one may conclude that the predominant effect of water vapor plasma treatment is the surface hydroxylation of the polyimide. This hydroxylation is most likely in the form of phenols and/or catechols.

Water vapor plasma surface modification provides a means of building thin film multilayer structures with excellent interfacial adhesion. Continued exploration of the new surface chemistry created by water vapor plasma treatment, and its associated properties, is planned.

REFERENCES

1. J. R. Rasmussen, E. R. Stedronsky, and G. M. Whitesides, *J. Am. Chem. Soc.,* **99,** 4736 (1977).
2. D. Briggs, D. M. Brewis, and M. B. Konieczo, *J. Mater. Sci.,* **11,** 1270 (1976).
3. J. R. Rasmussen, D. E. Bergbreiter, and G. M. Whitesides, *J. Am. Chem. Soc.,* **99,** 4746 (1977).
4. D. S. Everhart and C. N. Reilley, *Surf. Int. Anal.,* **3**(6), 258 (1981).
5. D. S. Everhart and C. N. Reilley, *Anal. Chem.,* **53,** 665 (1981).
6. D. S. Everhart and C. N. Reilley, *Surf. Int. Anal.,* **3**(3), 126 (1981).
7. D. Briggs, D. G. Rance, C. R. Kendall, and A. R. Blythe, *Polymer,* **21,** 895 (1980).
8. A. R. Blythe, D. Briggs, C. R. Kendall, D. G. Rance, and V. G. I. Vichy, *Polymer,* **19,** 1273 (1978).
9. D. Briggs and C. R. Kendall, *Polymer,* **20,** 1053 (1979).
10. L. J. Gerenser, J. F. Elman, M. G. Mason, and J. M. Pochan, *Polymer,* **26,** 1162 (1985).
11. T. Ogita, A. N. Ponomarev, S. Nishimoto, and T. Nagiya, *J. Macromol. Sci.-Chem. A,* **22**(8), 1135 (1985).
12. D. K. Owens, *J. Appl. Polym. Sci.,* **19,** 265 (1975).
13. D. T. Clark and A. Dilks, *J. Polym. Sci. Polym. Chem. Ed.,* **17,** 957 (1979).
14. D. T. Clark and A. Dilks, *J. Polym. Sci. Polym. Chem. Ed.,* **15,** 2321 (1977).
15. D. K. Owens, *J. Appl. Polym. Sci.,* **19,** 3315 (1975).
16. H. Yasuda, H. C. Marsh, S. Brandt, and C. N. Reilley, *J. Polym. Sci. Polym. Chem. Ed.,* **15,** 991 (1977).
17. D. Briggs, C. R. Kendall, A. R. Blythe, and A. B. Wooton, *Polymer,* **24,** 47 (1983).
18. A. Dilks, *J. Polym. Sci. Polym. Chem. Ed.,* **19,** 1319 (1981).
19. J. M. Burkstrand, *J. Vac. Sci. Technol.,* **15**(2), 223 (1978).
20. R. A. Dickie, J. S. Hammond, J. E. DeVries, and J. W. Holubka, *Anal. Chem.,* **54,** 2045 (1982).
21. D. T. Clark and A. Harrison, *J. Polym. Sci. Polym. Chem. Ed.,* **19,** 1945 (1981).
22. U.S. Pats. 4,382,101—"Method for Increasing the Peel Strength of Metal-Clad Polymers," by Anthony J. Polak, Lake Zurich, Ill., Assignor to UOP Inc., Des Plaines, Ill.—May 3, 1983; 4,765,860—"Method of Making a Flexible Base Plate for Printed Circuit Board," by Susumu Veno, Hajime Kitamura, Kaname Inoue—August 23, 1988; 4,755,424—"Polyimide Film

Having Improved Adhesive Properties," by Yoshiki Takeoa, Hideki Kawai, and Tsuneo Yamamoto—July 5, 1988; 4,740,282—"Hydrophilization of Hydrophobic Intraocular Lenses," by Hyman D. Gesser & Robert E. Warriner—April 26, 1988.

23. P. Blais, D. J. Carlsson, and D. M. Wiles, *J. Appl. Polym. Sci.,* **15,** 129 (1971).

24. M. Stradal and D. A. I. Goring, *Can. J. Chem. Eng.,* **53,** 427 (1975).

25. J. Freidrich and H. Frommelt, *Acta Chim. Hung.,* **125**(1), 165 (1988).

26. R. T. Haasch and J. F. Evans, *J. Vac. Sci. Technol. A,* **6**(3), 1074 (1988).

27. S. V. Korobtsev, T. A. Kosinova, V. A. Nesterov, Y. R. Rakhimbabaev, and V. D. Rusanov, *Sov. Phys. Tech. Phys.,* **29**(4), 619 (1984).

28. A. Rutscher and H. E. Wagner, *Int. Conf. Phenom. Ioniz. Gases,* **16**(4), 550 (1983).

29. K. Hiraoka, K. Morise, and T. Shoda, *Int. J. Mass Spectrom. Ion Process.,* **67,** 11 (1985).

30. Y. Ichikawa, T. Kaneda, R. M. Hobson, and J. Chang, *Res. Rep. Fac. Eng. Tokyo Denkai Univ.,* **29,** 15 (1981).

31. T. G. Vargo, J. A. Gardella, and L. Salvati, *J. Polym. Sci. Polym. Chem.,* **27,** 1267 (1989).

32. L. Salvati, T. J. Hook, J. A. Gardella, and R. L. Chin, *Polym. Eng. Sci.,* **27**(13), 939 (1987).

33. L. M. Ferreiro, D. W. Ernie, and J. F. Evans, *J. Vac. Sci. Technol. A,* **5**(4), 2280 (1987).

34. K. Nakamae, K. Yamaguchi, S. Tanigawa, K. Sumiya, and T. Matsumoto, *J. Chem. Soc. Jpn.,* **11,** 1995 (1987).

35. R. G. Nuzzo and G. Smolinsky, *Macromolecules,* **17,** 1013 (1984).

36. J. F. Evans, J. H. Gibson, J. F. Moulder, J. J. Ham-mond, and H. Goretzki, *Frez. Z. Anal. Chem.,* **319,** 841 (1984).

37. L. P. Buchwalter, B. D. Silverman, L. Witt, and A. Rossi, *J. Vac. Sci. Technol. A,* **5**(2), 226 (1987).

38. Y. Martin, C. C. Williams, and H. K. Wickramasinghe, *J. Appl. Phys.,* **61**(10), 4723 (1987).

39. N. J. Chou, A. D. Marwick, R. D. Goldblatt, L. Li, G. Coleman, J. E. Heidenreich, and J. R. Paraszczak, *J. Vac. Sci. Technol. A,* **10**(1), 248 (1992).

40. J. R. Bird and J. S. Williams, *Ion Beams for Materials Analysis,* Academic Press, San Diego, CA, 1989, p. 144.

41. D. Briggs, H. Chan, M. J. Hearn, D. I. McBriar, and H. S. Munro, *Langmuir,* **6,** 420 (1990).

42. T. Teraya, A. Takahara, and T. Kajiyama, *Polymer,* **31,** 1149 (1990).

43. D. G. LeGrand and G. L. Gaines, Jr., *J. Coll. Int. Sci.,* **31,** 162 (1969).

44. D. G. LeGrand and G. L. Gaines, Jr., *J. Coll. Int. Sci.,* **50,** 272 (1975).

45. W. W. Y. Lau and C. M. Burns, *J. Polym. Sci. Polym. Phys. Ed.,* **12,** 431 (1974).

46. J. N. Israelachvili, and M. L. Gee, *Langmuir,* **5,** 288 (1989).

47. E. Bayramli, T. G. M. van de Ven, and S. G. Mason, *Can. J. Chem.,* **59,** 1954 (1981).

48. T. S. Oh, S. P. Kowalczyk, D. J. Hunt, and J. Kim, *J. Adhes. Sci. Technol.,* **4,** 119 (1990).

49. M. M. Plechaty and R. R. Thomas, to appear.

50. J. Horkans, J. Kim, C. McGrath, and L. Romankiw, *J. Electrochem. Soc.,* **134,** 300 (1987).

51. J. Kim, S. H. Wen, D. Y. Jung, and R. W. Robinson, *IBM J. Res. Dev.,* **28,** 697 (1984).